ACCURACY ASSESSMENT OF RADARGRAMMETRIC DEMS DERIVED FROM RADARSAT-2 ULTRAFINE MODE

M. Ali DEMIR[a,]*, Elif SERTEL [b], Nebiye MUSAOGLU[b], Cankut ORMECI [b]

[a] ITU, Informatics Institute, Satellite Communication and Remote Sensing Programme, 80626 Maslak Istanbul, Turkey - alidemir@itu.edu.tr
[b] ITU, Geomatics Dept. Remote Sensing Div, 80626 Maslak Istanbul, Turkey – (sertele, musaoglune, cankut)@itu.edu.tr

Commission I, WG I/4

KEY WORDS: RADARSAT-2, Radargrammetric DEM, Accuracy, GDEM, Rational Function Model, Stereo SAR

ABSTRACT:

The aim of this study is to investigate the accuracy and reliability of radargrammetric DEMs generated from RADARSAT-2 stereo pairs. Two ultrafine mode images U7 and U26 were acquired over an area in Istanbul from descending orbit, HH polarization, in SGF format. U7 and U26 were taken on August 2, 2009 and July 30, 2009 with view angles of 34.0^0 - 35.3^0 and 48.5^0 - 49.5^0 at the near–far edges, respectively. The main project steps for DEM generation were; 1) Stereo model set up; 2) creating epipolar images; 3) image matching; 4) DEM editing. In order to set up the stereo model, ground control points (GCPs) were obtained from IKONOS image for planimetric information. Also 1:5000 scaled topographic maps were used for elevation information. After the setting up the stereo model with Toutin's 3D physical model developed at the Canada Centre for Remote Sensing (CCRS) and rational function model, radargrammetric DEMs were generated. Root mean square errors (RMSEs) of both GCPs and Independent Check Points (ICPs) were analyzed to evaulate the planimetric and elevation accuracy. Several transects were selected and elevation values obtained from Toutin's and rational function models were statistically compared with a reference DEM. Generated DEMs were also visually compared with Global Digital Elevation Model (GDEM).

1. INTRODUCTION

A Digital Elevation Model (DEM) is a digital representation of ground surface topography or terrain. DEMs can be generated using remote sensing techniques, field surveys and/or digitizing of topographical maps. However, remote sensing methods are superior to conventional methods since fast and economic data acquisition is possible with remote sensing. DEMs are currently one of the most important data used for geo-spatial analysis since subsequent information like slope, aspects etc. for various applications can be easily derived using DEMs. Common uses of DEMs include; rectification of aerial photography or satellite imagery, rendering of 3D visualizations, creation of slope, aspect and relief maps, modeling water flow or mass movement and extraction terrain parameters.

It is important to evaluate the accuracy of DEMs generated from satellite images since the accuracy of resulting DEM also impacts the accuracy and reliability of conducted analyses. Several researches have been conducted in recent years to investigate the accuracy of DEMs generated from optic and radar data (Toutin, 2002b; Toutin, 2004a; Cuartero et al., 2005; Oliviera et al., 2008; Peng et al., 2005; Chen et al., 2007).

Toutin, 2004a evaluated the elevation accuracy for digital surface model (DSM) generated from QuickBird stereo images using a three-dimensional (3D) physical model. He used 10 accurate ground control points (GCPs) to set up the stereo model and he found 1–2 m errors in the three axes with 48 independent Check Points. DSM was generated using an area-based multi-scale image matching method and then compared to light detection and ranging (LIDAR) elevation data with 0.2 m accuracy. An elevation error with 68% confidence level (LE68) of 6.4 m was achieved over the full area. Cuartero et al., 2005 investigated the reliability of SPOT HRV and Terra ASTER Digital Elevation Models. They generated 91 DEMs from SPOT data and 55 DEMs from ASTER data. To evaluate the accuracy of DEMs they used 315 Check Points determined by Differential Global Positioning systems. Results of Terra ASTER DEMs showed that RMSE (root mean square error) obtained for elevations is 13.0 m. The corresponding RMSE value for SPOT HRV DEM was 7.3 m. In both cases, the error was less than the pixel size. In addition to these researches, there are too many studies related to radargrammetric DEM from different SAR (Synthetic Aperture Radar) sensors in the literature (Oliviera et al., 2008; Peng et al., 2005; Chen et al., 2007; Toutin 2002b).

Although several DEM accuracy assessment studies could be found for different satellite sensors, there have not been comprehensive studies for RADARSAT-2 data. Toutin 2009, investigated the adaptation of Toutin's 3-D radargrammetric model and its application to RADARSAT-2 modes. He made several tests using different number of GCPs. The results were

* Corresponding Author: Muhammed Ali DEMİR, ITU, Civil Engineering Faculty, Geomatics Engineering Department, 34469 Maslak Istanbul, Turkey; E-mail: alidemir@itu.edu.tr

about 2 m for the 2-D positioning and 1 m in planimetry and 2 m in elevation for the 3-D positioning.

The aim of this study is to investigate the accuracy and reliability of radargrammetric DEMs over İstanbul which are generated from RADARSAT-2 stereo pairs using Toutin's 3D physical model developed at the Canada Centre for Remote Sensing (CCRS) and Rational Function Model (RFM). RMSE values of GCPs/ICPs, visual interpretation methods and statistical analysis were used for the accuracy assessment.

2. STUDY AREA AND DATA SET

The study site is approximately 20kmx20km located in Istanbul, Turkey (Fig. 1). The city lies over two continents namely Asia and Europe which is divided by Bosphorus Strait. The elevation of study area ranges from sea level to more than 320 m. The study site consists of urban-residential areas, rural environment, forest, sea, lakes and agricultural lands.

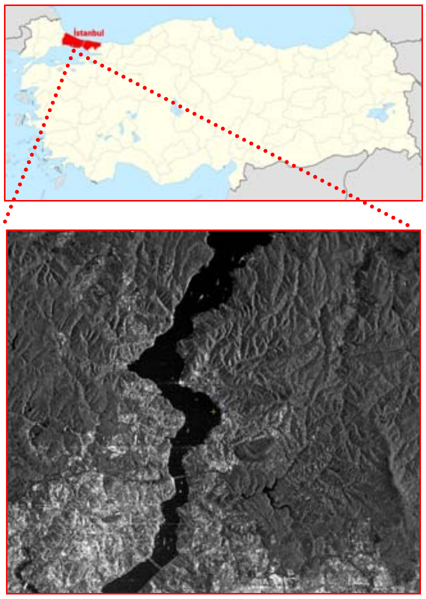

Figure 1. The study area - RADARSAT-2 U26 image

The RADARSAT-2 data set consisting two ultrafine mode images U7 and U26 (20x 20km^2, Fig. 1) were acquired over an area in Istanbul from descending orbit and HH polarization. U7 and U26 were received on August 2, 2009 and July 30, 2009 with view angles of 34.00 – 35.30 and 48.50 -49.50 at the near–far edges, respectively. The images were processed as SGF product (1x1 look; 1.56m pixel spacing).
Horizontal coordinates of GCPs were obtained from 1 m resolution IKONOS ortho-image of İstanbul which has approximately 1m accuracy. In addition, a reference DEM having 3 m grid size was created from 1:5000 scaled topographic maps was used for GCPs elevation values and accuracy assessment. For visual comparison GDEM (Global DEM) obtained from JPL web page. GDEM is a product of the Advanced Spaceborne Thermal Emission and Reflection Radiometer (ASTER), a joint program of NASA and Japan's Ministry of Economy, Trade and Industry. This data set was released on June 29, 2009, and was created by processing and stereo-correlating the 1.3 million-scene ASTER archive of optical images, covering Earth's land surface between 83 degrees North and 83 degrees South latitudes with estimated accuracies of 20 meters at 95 % confidence for vertical data and 30 meters at 95 % confidence for horizontal data (Smith, 2009; ASTER GDEM Validation Team, 2009).

3. METHODOLOGY

Satellite images can not be used directly as a map since they usually contain some geometric distortions due to the earth curvature and rotation, scan skew, mirror scan velocity, panoramic distortion, platform velocity and topography. The sources of these distortions can be grouped into two main categories: the observer or the acquisition system (platform, imaging sensor) and the observed (atmosphere and Earth). These distortions need to be corrected in order to derive accurate spatial information from satellite images. Mathematical and physical models are used to perform the geometric corrections of an image. Simply, these models identify geometric relationships between image space and object space.

In this study Toutin's 3D parametric (physical) model developed at CCRS and RFM were used to set up geometric and stereo model separately. Toutin's model (TM) is a 3D parametric model and was originally developed to suit the geometry of push-broom scanners (Toutin, 1995) and has been subsequently adapted as an integrated geometric modeling to multisensor, medium-high resolution optic and radar images. TM represents the well-known collinearity condition (and coplanarity condition for the stereo model) (Toutin, 1995). This model could mathematically model all distortions related to platform, the sensor and the Earth such as position and velocity of the platform, viewing angle of the sensor and Earth curvature. The geometric correction process can address each distortion separately or simultaneously (Toutin, 2004b). To compute the model parameters, image ephemeris data and GCPs are used in this model. TM is required fewer numbers of GCPs than non-parametric methods and not sensitive the distribution of GCPs in the image if there is no extrapolation in planimetry and elevation (Toutin and Chenier, 2009).

The second model used for DEM generation in this study is the Rational Function Model (RFM). This model is 3D non-parametric model and can be used when the parameters of the acquisition system or 3D parametric model are not available. A priori information on any component of the total system is not needed in this model, therefore it does not reflect platform, sensor, Earth and map projection related distortions (Toutin et al., 2002a). The following is a general form of 3D rational functions equation (Equation 1).

$$R_{3D}(XYZ) = \frac{\sum_{i=0}^{m}\sum_{j=0}^{n}\sum_{k=0}^{p} a_{ijk} X^i Y^j Z^k}{\sum_{i=0}^{m}\sum_{j=0}^{n}\sum_{k=0}^{p} b_{ijk} X^i Y^j Z^k} \qquad (1)$$

Where: X, Y, Z are the terrain coordinates; a_{ijk} and b_{ijk} are polynomial coefficients and called rational polynomial coefficients (RPCs); m, n, p are integer values and order of the polynomial functions.

RFMs can be divided into terrain-independent and terrain-dependent categories, considering if the physical sensor model is known or unknown. In this study only terrain-independent approach was used.

Terrain-independent approach is performed in two steps. At the first step, coefficients obtained from the already-solved existing 3D parametric model are used to define a 3D regular grid of the image terrain and compute the image coordinates of the 3D grid ground points. Then, 3D rational functions are resolved and the unknown parameters are computed using the GCPs obtained from grid points and their 3D ground and 2D image coordinates. As a result, DEM or ortho-images can be generated without colleting GCPs and post processing can be conducted using GCPs to improve accuracy of DEM or ortho-images (Toutin et al., 2002a). Thus, this approach is called terrain-independent.

3.1 Radargrammetric DEM Generation

The main processing steps for radargrammetric DEM generation are;

1. Stereo model setup
2. Creating epipolar images
3. Automatic image matching and 3D stereo intersection
4. DEM editing.

For DEM generation, the software of PCI Geomatica version 10.2 was used. The stereo model setup was computed with an iterative least squares bundle adjustment that enables the parameters of the geometric model to be refined with GCP's (Toutin, 2000) using both TM and RFM separately. Theoretically, six accurate GCPs are enough to compute the TM (Toutin and Chenier, 2009), however totally, 17 GCPs and 7 independent check points (ICPs) were collected to construct the model. Since TM is not sensitive the distribution of GCPs in the image, the distribution of GCPs was not taken into account but extrapolation limits were considered. Moreover, 29 tie points (TPs) were selected between two images (U26 and U27). Since RADARSAT-2 data are provided with the coefficients of 3-rd order RFM (numerical values of the 80RPCs) and RFM terrain-independent approach does not require any GCPs, only 8 (4 per images) GCPs were used to refine the stereo model results with 2D polynomial functions and geocode the DEM. Also 6 ICPs and 29 TPs were used for RFM.

Horizontal coordinates(X, Y) of all GCPs were obtained from 1m resolution ortho-mosaic İstanbul image and their elevation values (Z) obtained from a reference DEM which has 3 m grid size and approximately 1 m vertical accuracy.
After setting up the stereo model, epipolar images were generated. Since epipolar images reduce the errors between the stereo images in the y direction, correlation between the images is increased. Therefore, usage of epipolar images for DEM generation increases the speed of the image matching process and produces more accurate results. After this step, automatic DEM extraction was performed and two user defined geocoded DEMs were generated. These are; DEM1 derived from TM and DEM2 derived from RFM.

At the first step of DEM editing, İstanbul Bosphorus Strait, which is a water body, was masked and extracted from the generated DEMs. Afterwards, different filtering algorithms like noise, interpolation and smoothing filters were applied to DEMs to eliminate noise effect, remove artifacts and increase the comprehensibility.

Noise removal filter discards any artifacts left in the DEM and tends to remove small areas of noisy pixels. Two separate filters were applied during the noise removal process. The average and variance of the eight elevation values surrounding each pixel are calculated at the first stage. Failed and background pixels are excluded during the calculation. The center pixel is compared with the average and if it is two standard deviations or more away from the average, it is replaced with the failed value. The second filter counts up the number of failed values directly surrounding each pixel. If five or more failed pixels are found, the center pixel is assigned as a failed value (PCI Geomatics, 2007).

Interpolation filters are used to replace failed values with new elevation values which are interpolated from the good elevation values at the edges of the failed area. The interpolation algorithm can be osed for areas of 200 pixels or smaller. The smoothin of DEM was conducted with a 3 pixel by 3 pixel Gaussian smoothing filter. Pixels having failed or background values are ignored during the smoothing calculations (PCI Geomatics, 2007).

4. RESULTS

RMSEs of GCPs and ICPs were calculated and visual interpretation and statistical analysis were conducted for the accuracy assessment of radargrammetric DEMs (DEM1 and DEM2)

4.1 Analysis of GCPs/ICPs

Tables 1 shows the results of stereo model computed with an iterative least square bundle adjustment using both TM and RFM, respectively.

Residuals for TM				
	Number of Points	X_{RMSE} (m)	Y_{RMSE} (m)	$Total_{RMSE}$ (m)
GCPs	17	0.15	0.39	0.42
ICPs	7	1.19	1.25	1.73
TPs	29	0.09	0.34	0.35
Residuals for RFM				
	Number of Points	X_{RMSE} (m)	Y_{RMSE} (m)	$Total_{RMSE}$ (m)
GCPs	8	0.60	0.43	0.74
ICPs	6	2.84	1.08	3.04
TPs	29	0.57	0.31	0.65

Table 1. Root mean square (RMS) residuals (in meters) of stereo model setup

Total RMSE values of GCPs are better than ICPs for both TM and RFM with the values of 0.42 m and 0.74 m, respectively. The results showed that, TM and RFM had 1.73 m and 3.04 m horizontal (X, Y) accuracy for ICPs, respectively. Since ICPs were not used to calculate the model coefficients, they were considered to check the horizontal accuracy of the created DEMs. Considering the pixel size (1.55 m) of the stereo images, TM and RFM have RMSE values of 1 and 2 pixel, respectively. The results showed that TM has better horizontal accuracy than RFM.

4.2 Visual Interpretation

The elevation of study area ranges from sea level to more than 320 m since it has both coastal line and mountains. In this assessment step, GDEM accepted as a reference DEM and extracted DEMs were compared to it. Figure 2 shows DEM1 (derived from TM), DEM2 (derived from RFM) and GDEM of the study area. Visual interpretation of these DEMs demonstrated that radargrammetric DEMs derived from both TM and RFM could capture the general topographic features of the study area.

Red boxes within the figure 2 show the location of mountain areas where elevations are higher. It was observed that the highest regions of the study area are better represented in DEM1 compared to DEM2 when GDEM is taken as reference. Blue boxes within the figure 2 show the location of water surfaces where elevations are lower. It seems that both DEM1 and DEM2 could capture these features while compared with GDEM.

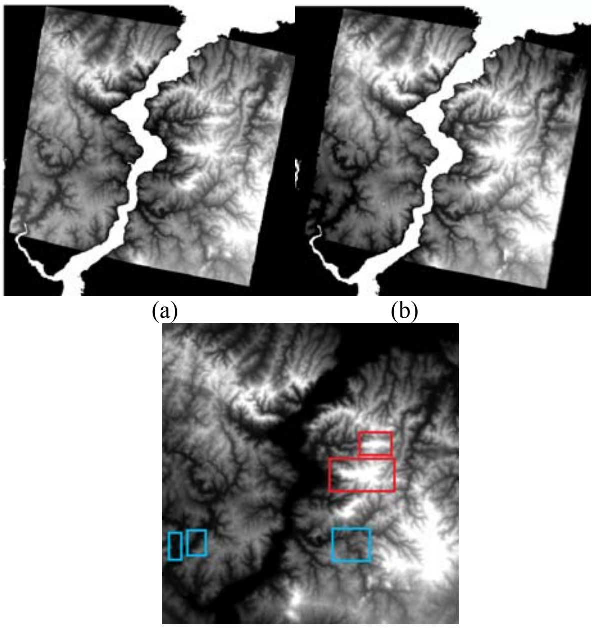

Figure 2. (a) DEM1, (b) DEM2, (c) GDEM. Red boxes are located over mountainous areas; blue boxes are located over water basin areas.

4.3 Statistical Analysis

In order to evaluate the accuracy of radargrammetric DEMs (DEM1 and DEM2) precisely, these DEMs were compared with a reference DEM derived from 1:5000 scaled topographic maps. The statistical analyses were employed using the comparison results over seven profiles. Minimum, maximum, and root mean square errors (RMSE) of all profiles were calculated based on the differences between related DEM and reference DEM.

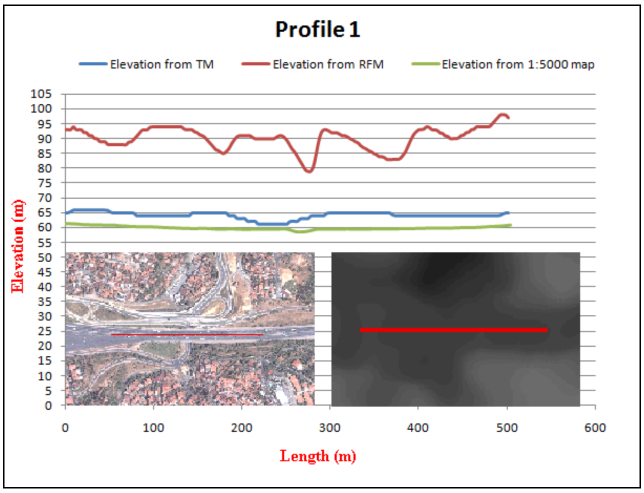

Figure 3. Location of Profile 1 and its elevation values

Profile 1 was selected from a highway where the elevation variations are not higher than 3-4 m according to reference DEM (Fig. 3). As can be seen in figure 3, DEM1 (Derived from TM) has close values to reference DEM values along this transect. In contrast, DEM2 (Derived from RFM) has significantly different values from reference DEM values. The minimum, maximum and root mean square errors obtained along this profile were; 1.61 m, 5.94 m, 4.61 m, for DEM1 and 27.85 m, 41 m and 34.57 m for DEM2, respectively.

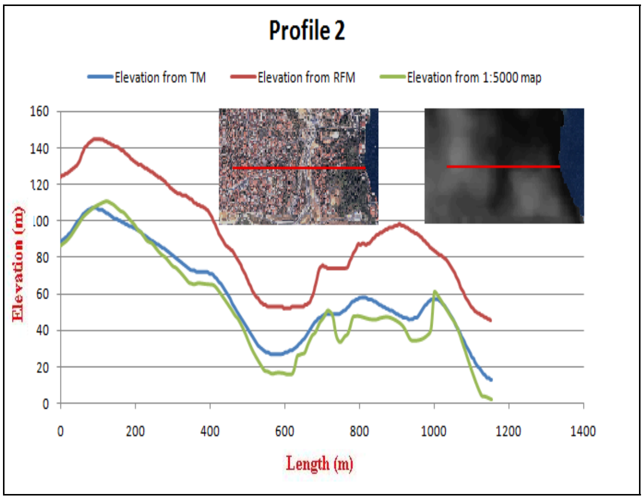

Figure 4. Location of Profile 2 and its elevation values

Profile 2 was selected from a residential area where the elevations range from sea level to 115m (Fig. 4). Although elevations of DEM1, DEM2 and reference DEM follow similar pattern, elevation values of DEM2 were significantly different from reference DEM values. Elevation values obtained from DEM1 and reference DEM gave similar results but there are some differences along the transect. The minimum, maximum and root mean square error value for this transect were; 0 m, 17.80 m, 7.56 m for DEM1 and 19.97 m, 60.39 m and 44.43 m for DEM2, respectively.

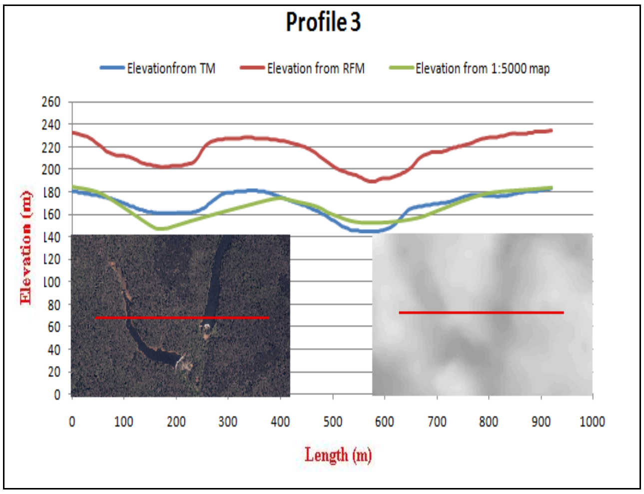

Figure 5. Location of Profile 3 and its elevation values

As can be seen in figure 5, profile 3 was selected along a forest area which also contains water surfaces. Although the fluctuations of DEM2 and reference DEM are similar to each other, DEM2 values are significantly different from reference DEM. DEM1 gives close results to reference DEM. Compared to reference DEM, the minimum, maximum and root mean square errors were; for DEM1 0.07 m, 15.85 m, 7.22 m, for DEM2 36.20 m, 64.96 m and 49.85 m, respectively.

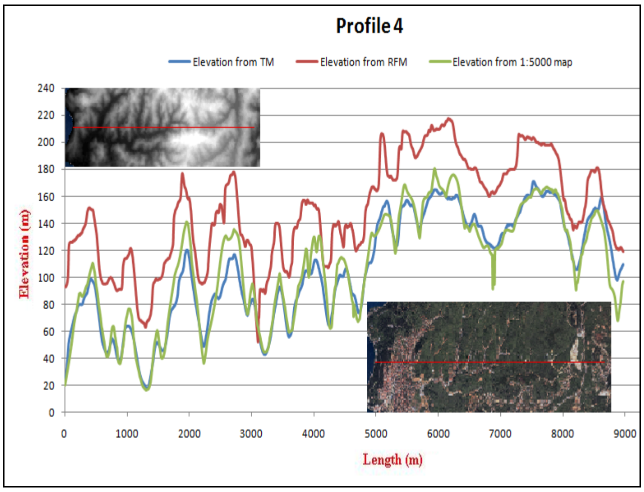

Figure 6. Location of Profile 4 and its elevation values

Profile 4 was selected over an area where different ranges of elevation are available (Fig. 6). DEM1 has similar values to reference DEM values but some peaks are not captured very well. Like previous profiles, DEM2 did not give the correct elevation values during the comparisos done with reference DEM. Compared to reference DEM, the minimum, maximum and root mean square errors were; for DEM1 0.01 m, 32.63 m, 10.43 m, for DEM2 0.16 m, 86.18 m and 42.18 m, respectively.

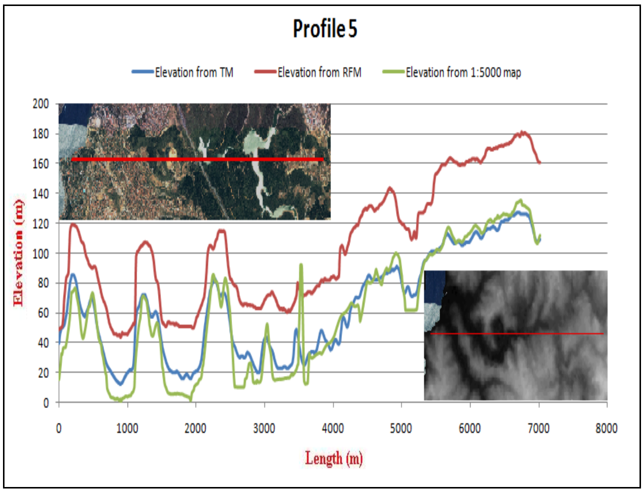

Figure 7. Location of Profile 5 and its elevation values

Profile 5 was selected from an area that consists of residential area, forest, water surface and highway (Fig. 7). Comparisons made between DEM1 and reference DEM showed that although the elevations of some part of this region were represented correctly with DEM1, there were 63 m difference between 3rd and 4th km of the transect. In addition, the lowest elevation values were not captured by DEM1. According to reference DEM, DEM2 gave very different results. Compared to reference DEM, the minimum, maximum and root mean square errors were; for DEM1 0 m, 63.63 m, 10.79 m, for DEM2 0.38 m, 68.84 m and 45.38 m, respectively

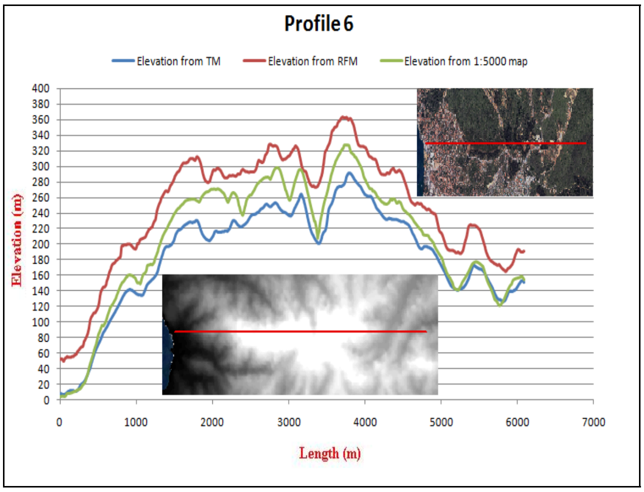

Figure 8. Location of Profile 6 and its elevation values

As can be seen in figure 8, profile 6 was selected from the highest region of study area. This transect lies over an elevation range of 4 m to 330 m. It can be obviously seen that DEM1 could not represent the high elevation values compared to reference DEM. Like previous profiles, DEM2 did not give acceptable results related to reference DEM. Compared to reference DEM, the minimum, maximum and root mean square errors were; for DEM1 0.01 m, 64.82 m, 26.54 m, for DEM2 4.73 m, 66.41 m and 40.55 m, respectively.

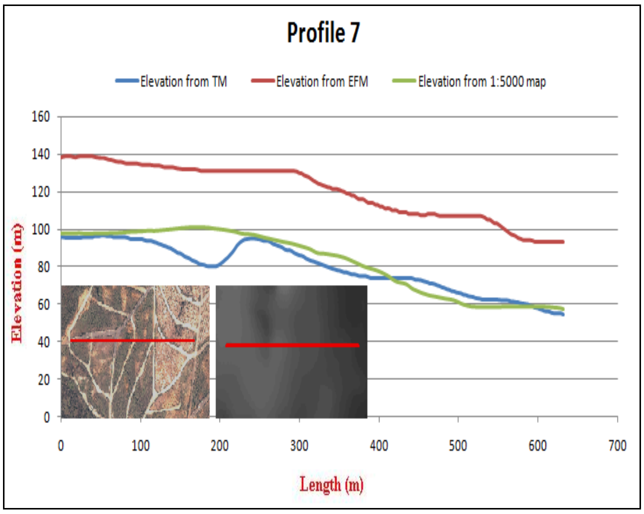

Figure 9. Location of Profile 7 and its elevation values

Profile 7 was selected from agricultural area where the elevations range 55 m to 102 m (Fig 9). Compared to reference DEM, the minimum, maximum and root mean square errors were; for DEM1 0.04 m, 20.69 m, 7.37 m, for DEM2 29.71 m, 48.40 m and 37.55 m, respectively.

5. CONCLUSION

In this study, two Digital Elevation Models were created using Toutin's 3D physical model (TM, DEM1) and Rational Functions Model (RFM, DEM2) by means of two Ultrafine beam mode RADARSAT-2 images of Istanbul. RFM model was refined with 2D polynomials to increase the horizontal accuracy of created DEM. Total RMSE values of TM and RFM derived DEMs were calculated as 0.42 m and 0.74 m for GCPs and 1.73 m (about 1 pixel) and 3.04 m (about 2 pixel) for ICPs, respectively. These RMSE values are the representation of horizontal accuracy.

A reference DEM generated from 1:5000 scaled topographic maps with approximately 1 m vertical accuracy was used to analyze the accuracy of DEM1 and DEM2. The minimum, maximum and RMSE values obtained from seven profiles were analyzed to examine the accuracy of generated DEMs. In most parts of the study region, DEM1 derived from TM has 10 m or better accuracy, however some parts of the region, especially the highest locations, error values were higher than 25 m considering the calculated maximum error values of 30 to 60 m. DEM2 derived from RFM, gave incoherent results when compared to DEM1 and reference DEM. At most parts of the study region, RMSEs of DEM2 are higher than 30 m and at some regions elevation difference between reference DEM2 and DEM reached up to 86 m. The differences obtained from DEM2 might be the biases resulting from vertical datum. Since RFM model uses coefficients coming with original RADARSAT-2 data and refinement was conducted for 2D, elevation values obtained from this DEM is not compatible with the reference DEM. Automatic usage of RFM for Turkey would not give reliable results because of the vertical datum problem. However, TM uses 3D GCPs and considers the vertical datum. Thus resulted in better results with TM.

6. REFERENCES

ASTER GDEM Validation Team, 2009. ASTER Global DEM Validation Summary Report. ASTER GDEM Validation Team: METI/ERSDAC NASA/LPDAAC USGS/EROS In cooperation with NGA and Other Collaborators.

Chen, Y., Shi, P., Li, J., Deng, L., Hu, D., Fan, Y., 2007. DEM accuracy comparison between different models from different stereo pairs. *International Journal of Remote Sensing,* 28 (19), 4217-4224.

Cuartero, A., Felicisimo, A. M., Ariza, F. J., 2005. Accuracy, Reliability, and Depuration of SPOT HRV and Terra ASTER Digital Elevation Models. *IEEE Transactions on Geoscience and Remote Sensing,* 43 (2), 404-407

Oliveira, C. G., Paradella, W. R., 2008. An Assessment of the Altimetric Information Derived from Spaceborne SAR (RADARSAT-1, SRTM3) and Optical (ASTER) Data for Cartographic Application in the Amazon Region*.* *Sensors*, 8, 3819-3829

PCI Geomatics: OrthoEngine User Guide, Canada, 2007

Peng, X., Wang, J., Zhang, Q., 2005. Deriving terrain and textural information from stereo RADARSAT data for mountainous land cover mapping. *International Journal of Remote Sensing,* 26 (22), 5029-5049

Smith, Y., 2009, "Global Digital Elevation Model", http://www.nasa.gov/multimedia/imagegallery/image_feature_1545.html (accessed 18 Sep. 2010).

TOUTIN, T., 1995*,* Generating DEM from stereo-images with a photogrammetric approach: examples with VIR and SAR data. *EARSeL Advances in Remote Sensing,* 4, 110–117.

Toutin, T., 2000. Evaluation of Radargrammetric DEM from RADARSAT Images in High Relief Areas. *IEEE Transactions on Geoscience and Remote Sensing,*38 (2).

Toutin, T., 2002b. Impact of terrain slope and aspect on radargrammetric DEM accuracy. *ISPRS Journal of Photogrammetry & Remote Sensing,* 57, 228– 240.

Toutin, T., 2004a. DSM Generation and Evaluation from QUICKBIRD Stereo Imaging with 3D Physical Modelling. *International Journal of Remote Sensing,* 25 (22), 5181-5193.

Toutin, T., 2004b. Review article Geometric processing of remote sensing images: models, algorithms and methods. *International Journal of Remote Sensing,* 25 (10), 1893–1924

Toutin, T., Chenier, R., 2009. 3-D Radargrammetric Modeling of RADARSAT-2 Ultrafine Mode: Preliminary Results of the Geometric Calibration. *IEEE Geoscience and Remote Sensing Letters,* 6 (3).

Toutin. T., Chenier, R., Carbonneau, Y., 2002a. 3D Models For High Resolution İmages: Examples With Quickbird, Ikonos And Eros. *Symposium Of Geospatil Theory Proccesing And Applications,* Ottowa